

# Geophysical Research Letters<sup>®</sup>



## RESEARCH LETTER

10.1029/2025GL118618

### Key Points:

- The ocean uptakes methyl chloroform (MCF) in the tropics and outgasses in the extratropics, the reverse of many other tracers such as CFC-11
- Our model estimates that the ocean outgassed 0.5 Gg yr<sup>-1</sup> of MCF in the 2010s, accounting for up to 30% of top-down inferred emissions
- This ocean outgassing is substantially larger than previous estimates and can significantly affect inferred MCF emissions and OH levels

### Supporting Information:

Supporting Information may be found in the online version of this article.

### Correspondence to:

P. Wang,  
[pdwang@mit.edu](mailto:pdwang@mit.edu)

### Citation:

Wang, P., Solomon, S., Scott, J. R., Yvon-Lewis, S. A., Wennberg, P. O., Weiss, R. F., et al. (2025). Ocean outgassing of methyl chloroform as an underestimated source of emission.

*Geophysical Research Letters*, 52, e2025GL118618. <https://doi.org/10.1029/2025GL118618>

Received 31 JUL 2025

Accepted 15 DEC 2025

## Ocean Outgassing of Methyl Chloroform as an Underestimated Source of Emission

Peidong Wang<sup>1,2</sup> , Susan Solomon<sup>1</sup> , Jeffery R. Scott<sup>1</sup> , Shari A. Yvon-Lewis<sup>3</sup> , Paul O. Wennberg<sup>4</sup> , Ray F. Weiss<sup>5</sup> , Matthew Rigby<sup>6,7</sup> , and Minde An<sup>7</sup>

<sup>1</sup>Department of Earth, Atmospheric and Planetary Sciences, Massachusetts Institute of Technology, Cambridge, MA, USA,

<sup>2</sup>Now at Doerr School of Sustainability, Stanford University, Stanford, CA, USA, <sup>3</sup>Department of Oceanography, Texas A&M University, College Station, TX, USA, <sup>4</sup>Division of Geological and Planetary Sciences, California Institute of Technology, Pasadena, CA, USA, <sup>5</sup>Scripps Institution of Oceanography, University of California San Diego, La Jolla, CA, USA, <sup>6</sup>School of Chemistry, University of Bristol, Bristol, UK, <sup>7</sup>Center for Sustainability Science and Strategy, Massachusetts Institute of Technology, Cambridge, MA, USA

**Abstract** Methyl chloroform (MCF) is an ozone-depleting substance used as an industrial solvent. Its primary sink is oxidation by the hydroxyl radical (OH), making it a key tracer for estimating atmospheric oxidative capacity. Following Montreal Protocol regulations, MCF emissions declined rapidly after the 1990s. However, the recent atmospheric MCF decay suggests persistent emissions and/or declining OH (contradicting chemistry-climate models projecting increasing or stable OH). The air-sea exchange of MCF has been poorly constrained due to limited observations and simplified ocean representations. We simulate oceanic MCF fluxes using a modern ocean reanalysis and validate with depth-resolved observations. Results suggest the ocean has shifted from a net sink to a net source around 2005, outgassing 0.5 Gg yr<sup>-1</sup> in the 2010s (up to 30% of inferred MCF emissions). This ocean outgassing is an order of magnitude larger than previous estimates, and accounts for up to a third of the model-observation discrepancy in OH.

**Plain Language Summary** Methyl chloroform (MCF) is a human-made compound that depletes stratospheric ozone, and its production has been phased out under the Montreal Protocol. However, recent observations show that atmospheric MCF is declining more slowly than expected, suggesting the presence of unexplained emissions and/or a decrease in hydroxyl radical (OH) levels (at odds with chemistry-climate models that suggest OH should have remained stable or increased). As anthropogenic MCF emissions have declined, the role of the ocean in both uptake and outgassing of MCF has grown more significant, but this component has been largely overlooked in previous studies. Here, we simulate ocean uptake and outgassing of MCF as accurately as current constraints allow. We find that the global ocean likely shifted to a net source of emission around 2005, releasing MCF at levels substantially higher than previously thought. Global OH levels are typically inferred from measurements of atmospheric MCF, which is primarily removed through reactions with OH, so changes in the MCF source strength in turn imply changes in inferred atmospheric OH. These results highlight the importance of accurately representing air-sea exchange in atmospheric trace gas budgets and inferences of OH levels.

## 1. Introduction

The hydroxyl radical (OH) is the primary atmospheric oxidant (Levy, 1971). OH governs the lifetimes of key greenhouse gases including methane (McNorton et al., 2016; Prather et al., 2012; Prather & Spivakovsky, 1990; Rigby et al., 2017; Turner et al., 2017) and various halocarbons (Liang et al., 2017; Prather & Spivakovsky, 1990; Rigby et al., 2013) (e.g., hydrochlorofluorocarbons [HCFCs] and hydrofluorocarbons [HFCs]), and it also influences air pollution through its role in tropospheric ozone chemistry (Levy, 1971; Singh et al., 1995). Therefore, accurately characterizing atmospheric OH is crucial for estimating greenhouse gas emissions as well as informing air pollution mitigation efforts. However, due to its extremely short atmospheric lifetime of about 1 s, OH cannot be directly measured on a global scale. Instead, global mean OH concentrations are most commonly inferred indirectly, from observations of atmospheric methyl chloroform ( $\text{CH}_3\text{CCl}_3$ ; MCF) (e.g., M. Krol & Lelieveld, 2003; Montzka et al., 2011; Naus et al., 2019; Patra et al., 2014; Prather et al., 2012; Prinn et al., 1992; Spivakovsky et al., 2000)—a relatively long-lived synthetic compound that has been globally monitored since 1978 (Prinn et al., 2018) and is predominantly removed by reaction with OH.

© 2025. The Author(s).

This is an open access article under the terms of the Creative Commons Attribution License, which permits use, distribution and reproduction in any medium, provided the original work is properly cited.

However, critical yet unresolved discrepancies remain between OH levels inferred from MCF using inverse modeling approaches and those simulated directly by process-based chemistry-climate models based on known OH chemistry. Process-based chemistry-climate models tend to overestimate absolute OH levels inferred from MCF by 10%–15% (Naik et al., 2013; Prather et al., 2012; Prinn et al., 2005). Chemistry-climate models also suggest stable or slightly increasing OH (Stevenson et al., 2020; Zhu et al., 2024), which conflicts with some MCF inverse modeling studies indicating a post-2005 decline (Rigby et al., 2017; Turner et al., 2017). Although process-based OH levels show substantial spread across models (Murray et al., 2021; Naik et al., 2013), MCF-based estimates can also carry large uncertainties and show differences between studies, raising concerns about their continued reliability for the inference of global OH (Nicely et al., 2020; Patra et al., 2021).

Inferring OH from MCF relies on knowledge of its source and sink terms. MCF is a stratospheric ozone-depleting substance and its anthropogenic emissions have declined rapidly due to controls of the Montreal Protocol (Laube & Tegtmeier, 2022). While bottom-up inventories provide well-constrained MCF production and emission estimates prior to 2000 (McCulloch & Midgley, 2001), they have been poorly characterized in the years since. To address this issue in quantifying OH, recent studies seek to simultaneously optimize both anthropogenic MCF emissions and OH concentrations in adjoint inversions (e.g., Naus et al., 2021; Rigby et al., 2017; Turner et al., 2017). However, other potential natural source and sink terms for MCF (i.e., from ocean uptake and outgassing) are proportionally increasing their significance as anthropogenic emissions have declined, introducing biases if these processes are poorly represented or overlooked in the inversion. Studies have suggested unexplained emissions occurring at least since 2013 (Naus et al., 2021; Rigby et al., 2017; Turner et al., 2017), when global MCF consumption should have ceased (Rigby et al., 2017). Based on atmospheric MCF measurements and a three-dimensional model inversion, a recent study attributed these unexplained emissions primarily to high latitudes and hypothesized that they could result from ocean outgassing, at a magnitude significantly larger than previous estimates (Naus et al., 2021). Those findings underscore the importance of quantitatively estimating oceanic MCF fluxes to assess their contributions to the atmospheric MCF budget and their impact on inferred global OH levels.

Oceanic uptake and outgassing of MCF have been rather ambiguously represented in previous OH inversions. MCF can dissolve in seawater and undergo further degradation through hydrolysis (Butler et al., 1991; Gerkens & Franklin, 1989; Yvon-Lewis & Butler, 2002). Earlier studies either neglect this process altogether or treat the ocean as a simple first-order loss term (Patra et al., 2011, 2014; Prather et al., 2012; Turner et al., 2017). A more complex, time-varying ocean uptake of MCF using an ocean general circulation model (Wennberg et al., 2004; hereafter W04) has only been incorporated in OH inversion studies recently (Patra et al., 2021; Rigby et al., 2017), and this oceanic term has been shown to be a dominant sensitivity factor for inferred OH (Rigby et al., 2017). However, W04 extends their projections of MCF air-sea fluxes beyond the 2000s, when atmospheric MCF observations were not available to constrain their model. Moreover, W04 uses the freshwater solubility of MCF, which may overestimate seawater uptake. Combined with limited ocean observations, their air-sea flux remains highly uncertain (Naus et al., 2021; Wennberg et al., 2004) and appears insufficient to account for the high-latitude source inferred in recent inversions (Naus et al., 2021; Rigby et al., 2017).

In this study, we simulate the ocean uptake and outgassing of MCF from 1992 to 2019 using the Estimating the Circulation and Climate of the Ocean (ECCO) framework (Forget, Campin, et al., 2015), which provides a physically consistent, observationally-constrained reconstruction of the global ocean. And by prescribing observed MCF atmospheric mole fractions from the Advanced Global Atmospheric Gases Experiment (AGAGE) network (Prinn et al., 2018), the model enables a realistic simulation of the oceanic uptake of MCF. A key strength of our study is the validation of simulated MCF distributions using an extensive set of depth-resolved ocean profile observations from a North Atlantic cruise conducted in July 2003 (A16N2003). We then evaluate the magnitude of ECCO-simulated MCF ocean outgassing relative to inferred total emissions, compare it with previous estimates, and discuss its potential implications for inferred OH abundances.

## 2. Materials and Methods

### 2.1. Sampling During the A16N2003 Cruise

Depth-resolved observations of CFC-11 and MCF were collected during the A16N2003 cruise aboard the National Oceanic and Atmospheric Administration (NOAA) R/V *Ronald H. Brown*, during June–August in 2003. Nearly all simultaneous measurements of CFC-11 and MCF were taken in July, spanning 44 stations from 45.5°N

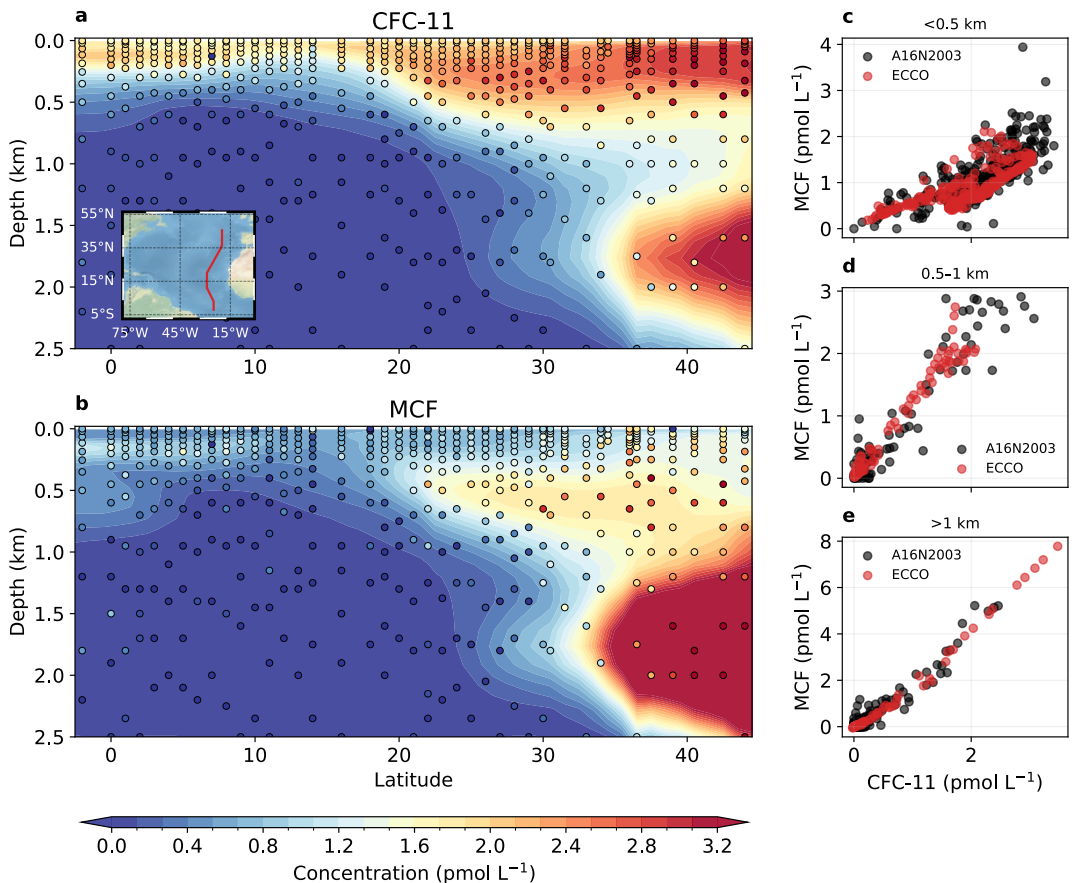


**Figure 1.** Validation of ECCO-simulated tracer distributions against observations. Panels (a and b) show vertical sections of CFC-11 and MCF concentrations along the A16N2003 cruise track. Observations are shown as colored dots and the cruise path is indicated by the red line in the map inset in panel (a). ECCO July monthly mean concentrations in 2003 are shown as colored shading, averaged longitudinally from 20°W to 29°W. Data below 2.5 km are omitted in (a, b) due to near-zero concentrations. Tracer-tracer scatter plots of observed and modeled CFC-11 versus MCF are shown in three depth ranges: above 0.5 km (c), 0.5–1 km (d), and 1–6 km (e). Black dots represent observations; red dots show ECCO output sampled at the nearest horizontal grid point and vertically interpolated to the observed depth. The strong agreement between ECCO and observed values indicates that the model realistically captures ocean tracer uptake and distributions for both CFC-11 and MCF.

to 2°S along longitudes 20°W to 29°W. The cruise track is shown in Figure 1a insert panel with the red line. During this cruise, over 600 data points were collected for each tracer, with maximum depth at ~5,900 m. Detailed descriptions of the measurement and sampling techniques are provided in Bullister and Gruber (2012) and Yvon-Lewis et al. (2004).

## 2.2. Ocean State Estimate and Atmospheric Forcing

The ocean state is represented by ECCO Version 4 Release 5 (Forget, Campin, et al., 2015), which assimilates satellite and in situ observations using the Massachusetts Institute of Technology General Circulation Model (MITgcm; Marshall, Adcroft, et al., 1997; Marshall, Hill, et al., 1997) to produce a physically consistent ocean reanalysis from 1992 to 2019. The ECCO simulation is run on the Lat-Lon-Cap 90 (LLC90) grid, with a horizontal resolution of approximately 1°, 50 vertical layers extending to ~6,100 m depth, and a time step of 1 hr. Modeled tracer concentrations and air-sea fluxes outputs are archived as monthly means, gridded on a regular 1° × 1° horizontal grid from the LLC90 grid.

We couple the ECCO ocean with monthly values of atmospheric mole fractions of CFC-11 and MCF from the AGAGE 12-box model output (Rigby et al., 2013). This 12-box model uses prior emission estimates for CFC-11 and MCF before 1978, and posterior emissions constrained by AGAGE observations thereafter. As a result, it

provides continuous monthly mole fractions for both species starting from a time when their atmospheric concentrations were effectively zero, allowing ocean accumulation to begin, and closely matches observations after 1978 (see Figures S1 and S2 in Supporting Information S1 for CFC-11 and MCF, respectively). The lower tropospheric mole fractions are provided across four latitude bands: 30°N–90°N, 30°N–equator, equator–30°S, and 30°S–90°S. To estimate spatially continuous air-sea fluxes, we linearly interpolate the atmospheric mole fractions every 10° of latitude across the boundaries of adjacent latitude bands (i.e., linearly interpolate from 35°N to 25°N, 5°N to 5°S, and 25°S to 35°S).

Because ECCO simulates time-varying ocean states that closely reflect observations only after 1992, we use the 1992 ocean state as a fixed boundary condition to estimate the initial distributions of CFC-11 and MCF. Specifically, we repeat the 1992 forcing fields in ECCO while prescribing time-varying atmospheric mole fractions starting from 1951 for both CFC-11 and MCF, allowing for tracer uptake and accumulation over time. This approach yields a reasonable estimate of the initial tracer distribution in the ocean by 1992. All results presented in this study focus on the period from 1992 onward.

Detailed descriptions of MCF solubility and hydrolysis, as well as air-sea exchange parameterizations, are provided in Texts S1 and S2 in Supporting Information S1.

### 2.3. Quantifying Changes in Inferred OH Associated With MCF Air-Sea Fluxes

We estimate the amount of inferred OH required to account for the air-sea MCF fluxes using the following equation:

$$\frac{dB}{dt} \Big|_{\text{ocn}} = -k \cdot \Delta OH \cdot B \quad (1)$$

where  $B$  is the total atmospheric burden of MCF (in Gg, derived from observed atmospheric mole fractions [in parts per trillion; ppt] by applying a scaling factor of 23.57 Gg ppt<sup>-1</sup>). This factor reflects the total atmospheric mass ( $5.1 \times 10^{18}$  kg), along with the molar masses of air (28.96 g mol<sup>-1</sup>) and MCF (133.4 g mol<sup>-1</sup>).  $\frac{dB}{dt}|_{\text{ocn}}$  represents the rate of change in atmospheric MCF burden (in Gg yr<sup>-1</sup>) due solely to air-sea exchange and is equivalent to the ocean uptake or outgassing of MCF. The reaction rate  $k$  corresponds to the temperature-dependent loss rate of MCF due to its reaction with OH, taken from Burkholder et al. (2019), assuming a mean tropospheric temperature of 266 K (as in Rigby et al., 2017).  $\Delta OH$  measures how much the inferred global mean OH abundance would need to account for the variations in atmospheric MCF burden caused by ocean-atmosphere exchange. This approach requires only the total atmospheric MCF burden (can be derived from observations) and the air-sea fluxes. Notably, it does not rely on MCF emission estimates, which are highly uncertain after 2000 (McCulloch & Midgley, 2001).

## 3. Results

We first validate the ECCO simulation of ocean tracer uptake using CFC-11, which is a well-characterized and nearly conserved compound that has long served as a passive tracer for studying ocean circulation (e.g., Beismann & Redler, 2003; L. Bullister & Weiss, 1983; Dutay et al., 2002; England et al., 1994; Ito et al., 2004; Romanou et al., 2017; Wanninkhof, 1992, 2014; Waugh, 2014). In this context, measured CFC-11, whose thermodynamic properties are well known for estimating ocean physical uptake and was not used in the ECCO state estimation, serves as independent evidence to test ECCO tracer uptake and distribution (Forget, Ferreira, & Liang, 2015). Importantly, both MCF and CFC-11 were measured simultaneously along the A16N2003 cruise, enabling a consistent tracer-tracer comparison. Figure 1 presents both the absolute concentrations and tracer-tracer scatter plots of CFC-11 and MCF from the ECCO simulation and the A16N2003 observation. The model broadly captures the observed latitudinal and depth distributions of both tracers, showing higher concentrations at high latitudes and in deeper waters, where surface solubility is elevated (due to lower temperatures) and where deep-water forms, facilitating tracer penetration.

The MCF results shown in Figure 1 represent our best estimate from the ECCO simulation after updating two key parameters from W04: solubility and hydrolysis rate (see Texts S1, S2 and Figure S4 in Supporting Information S1). Using the same freshwater solubility and hydrolysis rate for MCF as in W04 would lead to an

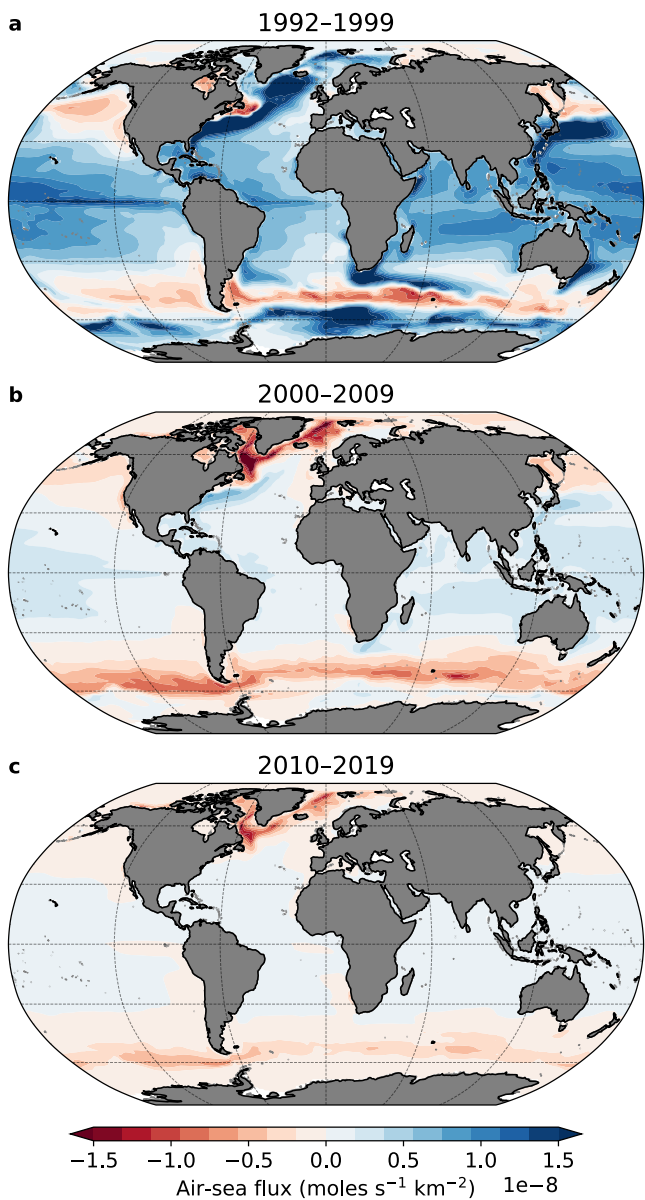


**Figure 2.** Spatial patterns of air-sea fluxes of MCF are shown as decadal averages for three time periods: 1992–1999 (a), 2000–2009 (b), and 2010–2019 (c). Positive values (blue) indicate ocean uptake; negative values (red) indicate ocean outgassing.

the first-order loss assumption becomes increasingly inadequate, particularly in later years, because it assumes the ocean is always a net sink and does not account for the possibility of outgassing.

The ECCO-simulated air-sea MCF flux, based on a time-varying ocean state, closely matches the W04 model, which uses a climatological ocean state, when the same freshwater solubility and hydrolysis rate parameters are applied (compare the blue solid and dashed lines in Figure 3a). This suggests that the oceanic MCF uptake is not strongly sensitive to the choice of ocean physical state. However, after accounting for seawater solubility and adopting a slower cold-temperature hydrolysis rate, the ocean acts as a significantly smaller reservoir for MCF—ocean uptake in the 1990s is reduced by more than 50%, and the onset of net outgassing occurs approximately 5 years in advance. This reduced ocean MCF uptake is driven primarily by the correction to seawater solubility, rather than adopting a slower hydrolysis rate, as demonstrated by additional sensitivity tests in Figure S7 in Supporting Information S1.

overestimation of ocean concentrations in the model (Figure S4 in Supporting Information S1 top row). However, updating the solubility based on a laboratory-measured salting-out coefficient (Gossett, 1987), while keeping the hydrolysis rate unchanged, shifts the modeled MCF concentrations toward the lower end of the observed range (Figure S4 in Supporting Information S1 middle row). However, we note that these hydrolysis losses of MCF were primarily extracted from rates measured at temperatures between 25°C and 120°C (Gerkens & Franklin, 1989), introducing substantial uncertainties in colder extratropical ocean waters (Naus et al., 2021; Wennberg et al., 2004). We find better agreement between the model and observations when the hydrolysis rate is reduced (i.e., slowed down), particularly at colder temperatures. Note this adjusted hydrolysis rate remains well within the reported uncertainty range (Gerkens & Franklin, 1989) (see Figure S3 in Supporting Information S1).

Figure 2 shows ECCO-simulated spatial distributions of air-sea MCF fluxes over the past three decades successively. In the 1990s, the global ocean acted predominantly as a sink for MCF across most regions. Since the 2000s, however, the tropics have remained a sink while the extratropical oceans are expected to have begun outgassing MCF. Intriguingly, this spatial flux pattern is opposite to that of many other trace gases, such as CFC-11, HCFCs, HFCs, and CO<sub>2</sub>, which are typically taken up by the ocean at high latitudes and released to the atmosphere in the tropics (DeVries et al., 2017; Gruber et al., 2009; Wang et al., 2021, 2023). This distinct pattern for MCF is primarily driven by its strong temperature-dependent hydrolysis in the ocean. Based on the hydrolysis parameters used in our simulation, MCF has a half-life on the order of less than a year in warm tropical waters (~25°C), but this extends to several decades in extratropical oceans where sea surface temperature drops below 10°C. As atmospheric MCF concentrations have declined rapidly under the Montreal Protocol, the tropical ocean remains undersaturated and continues to uptake MCF, due to rapid in situ degradation. In contrast, the extratropics become oversaturated and outgas MCF because of much slower chemical loss in the surface ocean.

To place our simulation in the context of earlier ocean representations, Figure 3a shows the globally integrated air-sea MCF flux for various ocean assumptions. Prior studies have often represented ocean uptake as a simple first-order loss process (e.g., assuming a constant oceanic partial lifetime of 197 years; Patra et al., 2011, 2014). Under this assumption, the oceanic loss in each year is calculated by simply dividing the atmospheric MCF burden by the oceanic partial lifetime. This approach provides a reasonable approximation in the 1990s, when the global ocean acted as a net sink for MCF, and uptake was largely driven by high atmospheric MCF burden due to large anthropogenic emissions. However, as emissions declined rapidly after the 1990s,

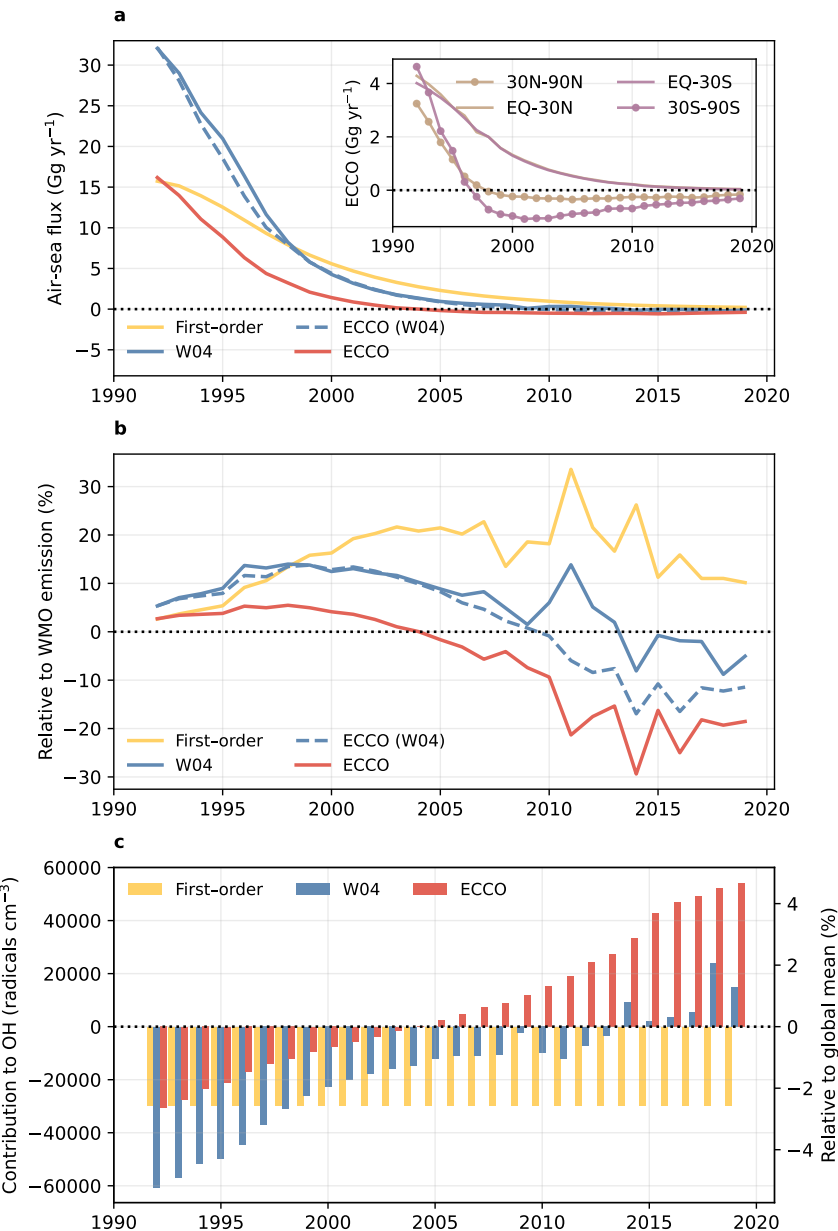


**Figure 3.** Time series of spatially integrated MCF air-sea fluxes and their impacts on inferred emissions and OH levels. Panel (a) shows comparison of global MCF air-sea fluxes from different ocean representations: first-order loss with an ocean partial lifetime of 197 years (yellow), an ocean general circulation model used in W04 (blue), and ECCO simulations in this study. The ECCO run using the same freshwater solubility and hydrolysis rate as W04 is shown as the blue dashed line. The best estimate from ECCO—corrected for seawater solubility and with a slower cold-temperature hydrolysis rate—is shown as the red solid line. The inset panel in (a) shows the ECCO best estimate air-sea fluxes of MCF separately integrated over four latitude bands: 30°N–90°N, 30°N–equator, equator–30°S, and 30°S–90°S. Positive values indicate ocean uptake, and negative values indicate ocean outgassing. Panel (b) shows the same air-sea fluxes data in (a) but relative to top-down MCF emissions inferred in the WMO 2022 Ozone Assessment report (Laube & Tegtmeier, 2022). Panel (c) shows the change in inferred OH that would be required to account for the air-sea MCF fluxes, if assuming the fluxes reflect changes in atmospheric MCF due to OH variations rather than atmosphere-ocean exchange (see Section 2.3 for details). The left y-axis indicates the absolute OH concentration (in radicals cm<sup>-3</sup>), and the right y-axis shows the corresponding relative change with respect to the global mean OH level of  $1.16 \times 10^6$  radicals cm<sup>-3</sup> (Spivakovsky et al., 2000).

Figure 3b compares the relative magnitude of various air-sea flux estimates to the top-down MCF emissions inferred in the World Meteorological Organization (WMO) 2022 Ozone Assessment report (Laube & Tegtmeier, 2022). In the 2010s, the inferred total MCF emissions were approximately  $2.9 \text{ Gg yr}^{-1}$ , even though reported

consumption had dropped to zero (Rigby et al., 2017). While this estimated MCF emission relies on a climatological OH field (Rigby et al., 2013; Spivakovsky et al., 2000)—and the values may vary somewhat depending on the assumed OH levels—the ECCO simulation estimates suggest that the global ocean outgasses about  $0.5 \text{ Gg yr}^{-1}$  of MCF back to the atmosphere, accounting for ~20% (and in some years up to 30%) of the inferred total emissions during the same period. It is also important to note that the top-down estimates in Figure 3b are based on a first-order ocean loss with a partial lifetime of 94 years (Laube & Tegtmeier, 2022; Yvon-Lewis & Butler, 2002), which assumes the ocean continued to act as a net sink for MCF in the 2010s (at  $\sim 1.0 \text{ Gg yr}^{-1}$ ), despite the possibility that it had already become a net source. As a result, this inferred land-based MCF emission (Laube & Tegtmeier, 2022) can be largely overestimated (by up to  $1.5 \text{ Gg yr}^{-1}$  in the 2010s).

Estimates of contributions to MCF-inferred OH due to different ocean representations are shown in Figure 3c. When the ocean acts as a net sink for MCF, accounting for air-sea fluxes lowers the inferred OH concentration because ocean uptake competes with OH as a sink for atmospheric MCF, reducing the amount of OH needed to balance the MCF mass budget. In contrast, when the ocean is a net source of MCF, including ocean outgassing increases the inferred OH level, since more OH is required to remove the additional MCF released from the ocean. To assess potential changes in inferred OH when using ECCO fluxes compared to earlier ocean representations, if one assumes that the ocean uptakes more MCF or only weakly outgasses MCF (e.g., W04 and first-order loss), but in reality the ocean uptakes less MCF before 2005 and outgasses more after 2005 (as simulated by ECCO), then the inferred OH levels would be higher when using ECCO fluxes than when using W04 or first-order loss assumptions (by as much as about 6% in recent years). This increase in inferred absolute OH abundance helps reduce the mismatch in which chemistry-climate models tend to overestimate OH by 10%–15% (Naik et al., 2013; Prather et al., 2012; Prinn et al., 2005). Similarly, ECCO indicates that the increasing ocean outgassing of MCF after 2005 would require the global mean OH trend to rise by about 3.5%/decade from 2005 to 2014. This boost in inferred OH due to consideration of ECCO-simulated ocean outgassing could partially reconcile the conflicting trends from previous MCF inversions (decreasing by about 6%/decade) versus chemistry-climate models (remaining stable or increasing) over the same period from 2005 to 2014 (Stevenson et al., 2020; Zhu et al., 2024). Note that this estimated impact of switching ocean representations on global mean OH assumes fixed emissions; part of the change in air-sea fluxes could instead offset MCF emissions if emissions and OH were jointly optimized.

#### 4. Summary and Discussion

We simulate MCF ocean uptake as accurately as current constraints allow—using an ocean state estimate from ECCO and prescribed observed atmospheric MCF mole fractions. In particular, by correcting for MCF seawater solubility as well as a slower cold-temperature hydrolysis rate, our modeled ocean MCF concentrations show good agreement with depth-resolved observations across a wide range of latitudes from a 2003 North Atlantic cruise. We find that in the 2010s, ocean outgassing of MCF from ECCO ( $\sim 0.5 \text{ Gg yr}^{-1}$ ) is substantially larger than previous estimates, based either on simple first-order loss assumptions (which suggest continued ocean uptake of up to  $\sim 1 \text{ Gg yr}^{-1}$ ) or on a time-varying ocean flux from W04 (which estimates outgassing at  $\sim 0.03 \text{ Gg yr}^{-1}$ ). This is qualitatively consistent with a recent inversion study (Naus et al., 2021), which suggested that a much larger high-latitude ocean source than W04 is needed to explain the observed intra-hemispheric gradient in atmospheric MCF mole fractions. Although the global ocean does not become a net source of MCF until after around 2005, the extratropical ocean appears to have begun outgassing as early as the late 1990s (Figure 3a, insert panel). This raises the possibility that changes in atmospheric MCF mole fractions previously attributed to European landfill emissions around the 2000s (Krol et al., 2003; Reimann et al., 2005) may instead reflect contributions from the ocean, particularly given that the subpolar North Atlantic emerges as a hot spot for ocean outgassing (Figures 2b and 2c).

As the observed decline in atmospheric MCF mole fractions slowed, previous inversion models that relied on smaller ocean outgassing estimates compensated for this bias by adjusting emissions to higher values, or invoking a decrease in atmospheric OH, or both, to balance the MCF mass budget. In contrast, ECCO indicates a large ocean source of MCF, potentially helping to explain the observed slowdown in the decay of atmospheric MCF mole fractions without invoking a substantial OH decrease or persistent emissions. Most importantly, our study suggests that the large MCF ocean source could account for as much as about 6% of the 10%–15% discrepancy between modeled and estimated absolute OH levels in recent years (Naik et al., 2013; Prather et al., 2012; Prinn et al., 2005).

Future inversion studies—particularly with three-dimensional atmospheric models (Naus et al., 2021; Patra et al., 2021) that incorporate spatially and temporally resolved MCF air-sea fluxes from ECCO or other ocean reanalyses—could offer additional insights into the spatiotemporal variability of OH. Such an approach would better disentangle oceanic and anthropogenic MCF sources and provide estimates of absolute OH concentrations across latitudes. Notably, process-based chemistry-climate models tend to produce larger hemispheric OH ratios than those inferred from MCF-based inversions (Naik et al., 2013; Patra et al., 2014; Stevenson et al., 2020). Our results show that the Southern Hemisphere outgasses roughly twice as much MCF as the Northern Hemisphere, indicating that accounting for hemispheric asymmetries in ocean fluxes of MCF may substantially affect inferred interhemispheric OH distributions. Although estimates of Southern Ocean outgassing can carry large uncertainties due to both the challenges of modeling its complex ventilation (Dutay et al., 2002) and the paucity of direct oceanic MCF measurements in this region. Frequent low-pressure storms over the Southern Ocean can further complicate estimates by altering total barometric pressure and, in turn, influencing air-sea gas exchange (Kelly et al., 2025). Additionally, our study adjusted the MCF hydrolysis rate at cold temperatures beyond the range of existing laboratory measurements to improve agreement between the model and observations. Future work that directly measures MCF hydrolysis rates under ocean-relevant conditions would help reduce these uncertainties, particularly for high latitudes.

With the rapid decline in MCF emissions, which have become poorly constrained in recent decades, OH inversion studies are also exploring alternative tracers, such as HCFCs and HFCs (Liang et al., 2017), CO (Chen et al., 2025) and CO isotope (Krol et al., 2008; Morgenstern et al., 2025), formaldehyde (Wells et al., 2020; Wolfe et al., 2019), and methane (Penn et al., 2025). While promising, these substitutes face several limitations: shorter observational records than MCF, more complex source and sink processes beyond OH, and some methods offer only regional rather than global constraints on OH. Given these challenges, accurately characterizing OH levels inferred from MCF remains important, as it can provide a valuable benchmark for evaluating OH estimates derived from alternative tracers. Accounting for air-sea exchange of MCF is critical for improving the fidelity of OH inversions—especially in recent years, when ocean outgassing may constitute a substantial fraction of the total source and thus introduce biases in top-down estimates if this process is neglected or highly simplified.

## Conflict of Interest

The authors declare no conflicts of interest relevant to this study.

## Data Availability Statement

A16N2003 cruise data is available at <https://www.pmel.noaa.gov/co2/story/A16N>. AGAGE atmospheric mole fractions data is available at <https://www-air.larc.nasa.gov/missions/agage/>. Gridded ECCO monthly air-sea fluxes, ocean concentrations for CFC-11 and MCF, and code used to generate all the figures in this analysis are available at Zenodo (Wang, 2025).

## Acknowledgments

P.W. gratefully acknowledges helpful discussions with Wei Chen, Qindan Zhu, and Gael Forget. S.S. and P.W. acknowledge support from the National Science Foundation Atmospheric Chemistry Division under Grant 2128617. S.A.Y. acknowledges support from the CLIVAR repeat hydrography program which is a joint effort between NOAA and NSF-OCE. M.R. received funding from the UK Natural Environment Research Council Highlight Topic, InHALE (Investigating HALOcarbon impacts on the global Environment; NE/X00452X/1) and the NASA Upper Atmosphere Research Program AGAGE Grant 80NSSC21K1369. The computations presented here were conducted using the “Svante” cluster, a facility located at MIT’s Massachusetts Green High Performance Computing Center and supported by the Center for Sustainable Science and Strategy (<https://cs3.mit.edu>).

## References

- Beismann, J.-O., & Redler, R. (2003). Model simulations of CFC uptake in North Atlantic Deep Water: Effects of parameterizations and grid resolution. *Journal of Geophysical Research*, 108(C5). <https://doi.org/10.1029/2001JC001253>
- Bullister, J. L., & Gruber, N. (2012). CRUISE REPORT: A16N\_2003a [Dataset]. [https://cchdo.ucsd.edu/cruise/33RO200306\\_01](https://cchdo.ucsd.edu/cruise/33RO200306_01)
- Bullister, J. L., & Weiss, R. F. (1983). Anthropogenic chlorofluoromethanes in the Greenland and Norwegian Seas. *Science*, 221(4607), 265–268. <https://doi.org/10.1126/science.221.4607.265>
- Burkholder, J. B., Sander, S. P., Abbatt, J., Barker, J. R., Cappa, C., Crounse, J. D., et al. (2019). *Chemical kinetics and photochemical data for use in atmospheric studies, Evaluation No. 19, JPL Publication 19-5*. Jet Propulsion Laboratory. Retrieved from <http://jpldataval.jpl.nasa.gov>
- Butler, J. H., Elkins, J. W., Thompson, T. M., Hall, B. D., Swanson, T. H., & Koropakov, V. (1991). Oceanic consumption of  $\text{CH}_3\text{CCl}_3$ : Implications for tropospheric OH. *Journal of Geophysical Research*, 96(D12), 22347–22355. <https://doi.org/10.1029/91JD02126>
- Chen, W., Zhang, Y., & Liang, R. (2025). Converging evidence for reduced global atmospheric oxidation in 2020. *National Science Review*, 12(8), nwaf232. <https://doi.org/10.1093/nsr/nwaf232>
- DeVries, T., Holzer, M., & Primeau, F. (2017). Recent increase in oceanic carbon uptake driven by weaker upper-ocean overturning. *Nature*, 542(7640), 215–218. <https://doi.org/10.1038/nature21068>
- Dutay, J.-C., Bullister, J. L., Doney, S. C., Orr, J. C., Najjar, R., Caldeira, K., et al. (2002). Evaluation of ocean model ventilation with CFC-11: Comparison of 13 global ocean models. *Ocean Modelling*, 4(2), 89–120. [https://doi.org/10.1016/s1463-5003\(01\)00013-0](https://doi.org/10.1016/s1463-5003(01)00013-0)
- England, M. H., Garçon, V., & Minster, J.-F. (1994). Chlorofluorocarbon uptake in a world ocean model: 1. Sensitivity to the surface gas forcing. *Journal of Geophysical Research*, 99(C12), 25215–25233. <https://doi.org/10.1029/94JC02205>
- Forget, G., Campin, J.-M., Heimbach, P., Hill, C. N., Ponte, R. M., & Wunsch, C. (2015). ECCO version 4: An integrated framework for nonlinear inverse modeling and global ocean state estimation. *Geoscientific Model Development*, 8(10), 3071–3104. <https://doi.org/10.5194/gmd-8-3071-2015>

- Forget, G., Ferreira, D., & Liang, X. (2015). On the observability of turbulent transport rates by Argo: Supporting evidence from an inversion experiment. *Ocean Science*, 11(5), 839–853. <https://doi.org/10.5194/os-11-839-2015>
- Gerkens, R. R., & Franklin, J. A. (1989). The rate of degradation of 1,1,1-trichloroethane in water by hydrolysis and dehydrochlorination. *Chemosphere*, 19(12), 1929–1937. [https://doi.org/10.1016/0045-6535\(89\)90016-7](https://doi.org/10.1016/0045-6535(89)90016-7)
- Gossett, J. M. (1987). Measurement of Henry's law constants for C1 and C2 chlorinated hydrocarbons. *Environmental Science & Technology*, 21(2), 202–208. <https://doi.org/10.1021/es00156a012>
- Gruber, N., Gloor, M., Mikaloff Fletcher, S. E., Doney, S. C., Dutkiewicz, S., Follows, M. J., et al. (2009). Oceanic sources, sinks, and transport of atmospheric CO<sub>2</sub>. *Global Biogeochemical Cycles*, 23(1). <https://doi.org/10.1029/2008GB003349>
- Ito, T., Marshall, J., & Follows, M. (2004). What controls the uptake of transient tracers in the Southern Ocean? *Global Biogeochemical Cycles*, 18(2). <https://doi.org/10.1029/2003gb002103>
- Kelly, C. L., Chang, B. X., Emmanuelli, A. F., Park, E. R., Macdonald, A. M., & Nicholson, D. P. (2025). Low-pressure storms drive nitrous oxide emissions in the Southern Ocean. *Research Square*. <https://doi.org/10.21203/rs.3.rs-6378208/v1>
- Krol, M., & Lelieveld, J. (2003). Can the variability in tropospheric OH be deduced from measurements of 1,1,1-trichloroethane (methyl chloroform)? *Journal of Geophysical Research*, 108(D3). <https://doi.org/10.1029/2002JD002423>
- Krol, M. C., Lelieveld, J., Oram, D. E., Sturrock, G. A., Penkett, S. A., Brenninkmeijer, C. A. M., et al. (2003). Continuing emissions of methyl chloroform from Europe. *Nature*, 421(6919), 131–135. <https://doi.org/10.1038/nature01311>
- Krol, M. C., Meirink, J. F., Bergamaschi, P., Mak, J. E., Lowe, D., Jöckel, P., et al. (2008). What can <sup>14</sup>CO measurements tell us about OH? *Atmospheric Chemistry and Physics*, 8(16), 5033–5044. <https://doi.org/10.5194/acp-8-5033-2008>
- Laube, J. C., & Tegtmeier, S. (2022). *Scientific assessment of ozone depletion: 2022. Chapter 1: Update on ozone-depleting substances (ODSs) and other gases of interest to the Montreal protocol* (No. 278) (p. 509). World Meteorological Organization.
- Levy, H. (1971). Normal atmosphere: Large radical and formaldehyde concentrations predicted. *Science*, 173(3992), 141–143. <https://doi.org/10.1126/science.173.3992.141>
- Liang, Q., Chipperfield, M. P., Fleming, E. L., Abraham, N. L., Braesicke, P., Burkholder, J. B., et al. (2017). Deriving global OH abundance and atmospheric lifetimes for long-lived gases: A search for CH<sub>3</sub>CCl<sub>3</sub> alternatives. *Journal of Geophysical Research: Atmospheres*, 122(21), 11914–11933. <https://doi.org/10.1002/2017JD026926>
- Marshall, J., Adcroft, A., Hill, C., Perelman, L., & Heisey, C. (1997). A finite-volume, incompressible Navier Stokes model for studies of the ocean on parallel computers. *Journal of Geophysical Research*, 102(C3), 5753–5766. <https://doi.org/10.1029/96jc02775>
- Marshall, J., Hill, C., Perelman, L., & Adcroft, A. (1997). Hydrostatic, quasi-hydrostatic, and nonhydrostatic ocean modeling. *Journal of Geophysical Research*, 102(C3), 5733–5752. <https://doi.org/10.1029/96jc02776>
- McCulloch, A., & Midgley, P. M. (2001). The history of methyl chloroform emissions: 1951–2000. *Atmospheric Environment*, 35(31), 5311–5319. [https://doi.org/10.1016/S1352-2310\(01\)00306-5](https://doi.org/10.1016/S1352-2310(01)00306-5)
- McNorton, J., Chipperfield, M. P., Gloor, M., Wilson, C., Feng, W., Hayman, G. D., et al. (2016). Role of OH variability in the stalling of the global atmospheric CH<sub>4</sub> growth rate from 1999 to 2006. *Atmospheric Chemistry and Physics*, 16(12), 7943–7956. <https://doi.org/10.5194/acp-16-7943-2016>
- Montzka, S. A., Krol, M., Dlugokencky, E., Hall, B., Jöckel, P., & Lelieveld, J. (2011). Small interannual variability of global atmospheric hydroxyl. *Science*, 331(6013), 67–69. <https://doi.org/10.1126/science.1197640>
- Morgenstern, O., Moss, R., Manning, M., Zeng, G., Schaefer, H., Usoskin, I., et al. (2025). Radiocarbon monoxide indicates increasing atmospheric oxidizing capacity. *Nature Communications*, 16(1), 249. <https://doi.org/10.1038/s41467-024-55603-1>
- Murray, L. T., Fiore, A. M., Shindell, D. T., Naik, V., & Horowitz, L. W. (2021). Large uncertainties in global hydroxyl projections tied to fate of reactive nitrogen and carbon. *Proceedings of the National Academy of Sciences*, 118(43), e2115204118. <https://doi.org/10.1073/pnas.2115204118>
- Naik, V., Voulgarakis, A., Fiore, A. M., Horowitz, L. W., Lamarque, J.-F., Lin, M., et al. (2013). Preindustrial to present-day changes in tropospheric hydroxyl radical and methane lifetime from the atmospheric chemistry and climate model intercomparison project (ACCMIP). *Atmospheric Chemistry and Physics*, 13(10), 5277–5298. <https://doi.org/10.5194/acp-13-5277-2013>
- Naus, S., Montzka, S. A., Pandey, S., Basu, S., Dlugokencky, E. J., & Krol, M. (2019). Constraints and biases in a tropospheric two-box model of OH. *Atmospheric Chemistry and Physics*, 19(1), 407–424. <https://doi.org/10.5194/acp-19-407-2019>
- Naus, S., Montzka, S. A., Patra, P. K., & Krol, M. C. (2021). A three-dimensional-model inversion of methyl chloroform to constrain the atmospheric oxidative capacity. *Atmospheric Chemistry and Physics*, 21(6), 4809–4824. <https://doi.org/10.5194/acp-21-4809-2021>
- Nicely, J. M., Duncan, B. N., Hanisco, T. F., Wolfe, G. M., Salawitch, R. J., Deushi, M., et al. (2020). A machine learning examination of hydroxyl radical differences among model simulations for CCM1-1. *Atmospheric Chemistry and Physics*, 20(3), 1341–1361. <https://doi.org/10.5194/acp-20-1341-2020>
- Patra, P. K., Houweling, S., Krol, M., Bousquet, P., Belikov, D., Bergmann, D., et al. (2011). TransCom model simulations of CH<sub>4</sub> and related species: Linking transport, surface flux and chemical loss with CH<sub>4</sub> variability in the troposphere and lower stratosphere. *Atmospheric Chemistry and Physics*, 11(24), 12813–12837. <https://doi.org/10.5194/acp-11-12813-2011>
- Patra, P. K., Krol, M. C., Montzka, S. A., Arnold, T., Atlas, E. L., Lintner, B. R., et al. (2014). Observational evidence for interhemispheric hydroxyl-radical parity. *Nature*, 513(7517), 219–223. <https://doi.org/10.1038/nature13721>
- Patra, P. K., Krol, M. C., Prinn, R. G., Takigawa, M., Mühlé, J., Montzka, S. A., et al. (2021). Methyl chloroform continues to constrain the hydroxyl (OH) variability in the troposphere. *Journal of Geophysical Research: Atmospheres*, 126(4), e2020JD033862. <https://doi.org/10.1029/2020JD033862>
- Penn, E., Jacob, D. J., Chen, Z., East, J. D., Sulprizio, M. P., Bruhwiler, L., et al. (2025). What can we learn about tropospheric OH from satellite observations of methane? *Atmospheric Chemistry and Physics*, 25(5), 2947–2965. <https://doi.org/10.5194/acp-25-2947-2025>
- Prather, M. J., Holmes, C. D., & Hsu, J. (2012). Reactive greenhouse gas scenarios: Systematic exploration of uncertainties and the role of atmospheric chemistry. *Geophysical Research Letters*, 39(9). <https://doi.org/10.1029/2012GL051440>
- Prather, M. J., & Spivakovsky, C. M. (1990). Tropospheric OH and the lifetimes of hydrochlorofluorocarbons. *Journal of Geophysical Research*, 95(D11), 18723–18729. <https://doi.org/10.1029/JD095iD11p18723>
- Prinn, R. G., Cunnold, D., Simmonds, P., Alyea, F., Boldi, R., Crawford, A., et al. (1992). Global average concentration and trend for hydroxyl radicals deduced from ALE/GAGE trichloroethane (methyl chloroform) data for 1978–1990. *Journal of Geophysical Research*, 97(D2), 2445–2461. <https://doi.org/10.1029/91JD02755>
- Prinn, R. G., Huang, J., Weiss, R. F., Cunnold, D. M., Fraser, P. J., Simmonds, P. G., et al. (2005). Evidence for variability of atmospheric hydroxyl radicals over the past quarter century. *Geophysical Research Letters*, 32(7). <https://doi.org/10.1029/2004GL022228>

- Prinn, R. G., Weiss, R. F., Arduini, J., Arnold, T., DeWitt, H. L., Fraser, P. J., et al. (2018). History of chemically and radiatively important atmospheric gases from the advanced global atmospheric gases experiment (AGAGE). *Earth System Science Data*, 10(2), 985–1018. <https://doi.org/10.5194/esd-10-985-2018>
- Reimann, S., Manning, A. J., Simmonds, P. G., Cunnold, D. M., Wang, R. H. J., Li, J., et al. (2005). Low European methyl chloroform emissions inferred from long-term atmospheric measurements. *Nature*, 433(7025), 506–508. <https://doi.org/10.1038/nature03220>
- Rigby, M., Montzka, S. A., Prinn, R. G., White, J. W. C., Young, D., O'Doherty, S., et al. (2017). Role of atmospheric oxidation in recent methane growth. *Proceedings of the National Academy of Sciences*, 114(21), 5373–5377. <https://doi.org/10.1073/pnas.1616426114>
- Rigby, M., Prinn, R. G., O'Doherty, S., Montzka, S. A., McCulloch, A., Harth, C. M., et al. (2013). Re-evaluation of the lifetimes of the major CFCs and  $\text{CH}_3\text{CCl}_3$  using atmospheric trends. *Atmospheric Chemistry and Physics*, 13(5), 2691–2702. <https://doi.org/10.5194/acp-13-2691-2013>
- Romanou, A., Marshall, J., Kelley, M., & Scott, J. (2017). Role of the ocean's AMOC in setting the uptake efficiency of transient tracers. *Geophysical Research Letters*, 44(11), 5590–5598. <https://doi.org/10.1002/2017gl072972>
- Singh, H. B., Kanakidou, M., Crutzen, P. J., & Jacob, D. J. (1995). High concentrations and photochemical fate of oxygenated hydrocarbons in the global troposphere. *Nature*, 378(6552), 50–54. <https://doi.org/10.1038/378050a0>
- Spivakovsky, C. M., Logan, J. A., Montzka, S. A., Balkanski, Y. J., Foreman-Fowler, M., Jones, D. B. A., et al. (2000). Three-dimensional climatological distribution of tropospheric OH: Update and evaluation. *Journal of Geophysical Research*, 105(D7), 8931–8980. <https://doi.org/10.1029/1999JD901006>
- Stevenson, D. S., Zhao, A., Naik, V., O'Connor, F. M., Tilmes, S., Zeng, G., et al. (2020). Trends in global tropospheric hydroxyl radical and methane lifetime since 1850 from AerChemMIP. *Atmospheric Chemistry and Physics*, 20(21), 12905–12920. <https://doi.org/10.5194/acp-20-12905-2020>
- Turner, A. J., Frankenberg, C., Wennberg, P. O., & Jacob, D. J. (2017). Ambiguity in the causes for decadal trends in atmospheric methane and hydroxyl. *Proceedings of the National Academy of Sciences*, 114(21), 5367–5372. <https://doi.org/10.1073/pnas.1616020114>
- Wang, P. (2025). Data and code for "Ocean outgassing of methyl chloroform as an underestimated source of emission" (Version 2) [Dataset]. *Zenodo*. <https://doi.org/10.5281/zenodo.16648860>
- Wang, P., Scott, J. R., Solomon, S., Marshall, J., Babbin, A. R., Lickley, M., et al. (2021). On the effects of the ocean on atmospheric CFC-11 lifetimes and emissions. *Proceedings of the National Academy of Sciences*, 118(12), e2021528118. <https://doi.org/10.1073/pnas.2021528118>
- Wang, P., Solomon, S., Lickley, M., Scott, J. R., Weiss, R. F., & Prinn, R. G. (2023). On the influence of hydroxyl radical changes and ocean sinks on estimated HCFC and HFC emissions and banks. *Geophysical Research Letters*, 50(18), e2023GL105472. <https://doi.org/10.1029/2023GL105472>
- Wanninkhof, R. (1992). Relationship between wind speed and gas exchange over the ocean. *Journal of Geophysical Research*, 97(C5), 7373–7382. <https://doi.org/10.1029/92JC00188>
- Wanninkhof, R. (2014). Relationship between wind speed and gas exchange over the ocean revisited. *Limnology and Oceanography: Methods*, 12(6), 351–362. <https://doi.org/10.4319/lom.2014.12.351>
- Waugh, D. W. (2014). Changes in the ventilation of the southern oceans. *Philosophical Transactions of the Royal Society A: Mathematical, Physical and Engineering Sciences*, 372(2019), 20130269. <https://doi.org/10.1098/rsta.2013.0269>
- Wells, K. C., Millet, D. B., Payne, V. H., Deventer, M. J., Bates, K. H., de Gouw, J. A., et al. (2020). Satellite isoprene retrievals constrain emissions and atmospheric oxidation. *Nature*, 585(7824), 225–233. <https://doi.org/10.1038/s41586-020-2664-3>
- Wennberg, P. O., Peacock, S., Randerson, J. T., & Bleck, R. (2004). Recent changes in the air-sea gas exchange of methyl chloroform. *Geophysical Research Letters*, 31(16). <https://doi.org/10.1029/2004GL020476>
- Wolfe, G. M., Nicely, J. M., St. Clair, J. M., Hanisco, T. F., Liao, J., Oman, L. D., et al. (2019). Mapping hydroxyl variability throughout the global remote troposphere via synthesis of airborne and satellite formaldehyde observations. *Proceedings of the National Academy of Sciences*, 116(23), 11171–11180. <https://doi.org/10.1073/pnas.1821661116>
- Yvon-Lewis, S. A., & Butler, J. H. (2002). Effect of oceanic uptake on atmospheric lifetimes of selected trace gases. *Journal of Geophysical Research*, 107(D20), ACH1-1–ACH1-9. <https://doi.org/10.1029/2001JD001267>
- Yvon-Lewis, S. A., King, D. B., Tokarczyk, R., Goodwin, K. D., Saltzman, E. S., & Butler, J. H. (2004). Methyl bromide and methyl chloride in the Southern Ocean. *Journal of Geophysical Research*, 109(C2). <https://doi.org/10.1029/2003JC001809>
- Zhu, Q., Fiore, A. M., Correa, G., Lamarque, J.-F., & Worden, H. (2024). The impact of internal climate variability on OH trends between 2005 and 2014. *Environmental Research Letters*, 19(6), 064032. <https://doi.org/10.1088/1748-9326/ad4b47>